ARTICLE NO. 79-1175R

J80-154

Ignition of Solid Propellant Crack Tip under Rapid Pressurization

60003

Mridul Kumar* and Kenneth K. Kuo†
The Pennsylvania State University, University Park, Pa.

Under rapid chamber pressurization rates ($\sim 10^5$ atm/s or higher), the closed end of a solid propellant crack was observed to ignite prior to the arrival of the convective ignition front. Tests were conducted in an inert crack with propellant only at the tip to eliminate some of the possible mechanisms for crack-tip ignition. Ignition delay time, defined as the time lag between the arrival of the pressure wave at the tip and the subsequent onset of emission of luminous light from the propellant surface, has been measured as a function of chamber pressurization rate. A theoretical model has been developed to explain the tip ignition phenomena. The model considers: a one-dimensional transient heat conduction equation for the solid phase; one-dimensional, unsteady mass and energy conservation equations for the gas phase near the crack tip; and an experimentally observed pressure-time trace near the crack-tip region in place of the gas phase momentum equation. Both experimental and theoretical results indicate that the ignition delay time decreases as the pressurization rate is increased. Theoretically calculated ignition delay times are in good agreement with the experimental data. Based upon this agreement, ignition near the crack-tip region is considered to be caused by the enhanced turbulent transport of energy in the gas phase, which is driven by strong compression waves.

Nomenclature

A = axial transformation constant for the gaseous region, cm^{-1}
A_l = axial transformation constant for the solid region, cm^{-1}
c_p = specific heat at constant pressure, cal/g-K
h = enthalpy of gas, $h=\tilde{h}+h''$, cal/g
k = thermal conductivity, cal/cm-s-K
k_{eff} = $k+k_t$, cal/cm-s-K
M_w = molecular weight, g_f/g-mole
P = pressure, $P=\bar{P}+P'$, g_f/cm^2
Pr = Prandtl number
$\dot{q}_w$ = heat flux at the propellant surface, cal/cm^2-s
R = specific gas constant for the combustion gases, g_f-cm/g-K
T = temperature (without subscript, gas temperature), K
T_f = adiabatic flame temperature, K
T_{pi} = initial propellant temperature, K
T_{ps} = propellant surface temperature, K
t = time, s
u = instantaneous gas velocity, $u=\tilde{u}+u''$, cm/s
x = axial coordinate, measured from propellant surface, cm
z = transformed nondimensional axial coordinate
α = thermal diffusivity, cm^2/s
γ = ratio of specific heats
δ = gap width of crack, cm
μ = gas viscosity, g/cm-s
ρ = density (without subscript, gas density), g/cm^3
ϕ = dissipation, cal/cm^3-s

Subscripts

eff = effective
i = initial value
ign = ignition condition
p = propellant
t = turbulent

Superscripts

$(\tilde{\ })$ = Favre or mass-averaged quantity
$(\bar{\ })$ = Reynolds or time-averaged quantity
$(\ )'$ = fluctuating quantities in Reynolds average method
$(\ )''$ = fluctuating quantities in Favre's average method

I. Introduction

A VERY important characteristic of a gas permeable solid propellant is that it undergoes the transition from normal burning to detonation under certain operating conditions. A transition from deflagration to detonation (DDT) may not only cuase malfunction or failure of a solid propellant motor, but it is also a potential source of hazard. DDT usually involves very high flame propagation rates, high pressures, and large burning surface areas. DDT is therefore more likely to occur in gas permeable propellants, such as granular propellant beds or propellant grains with flaws or cracks which have large burning surface areas. Various possible mechanisms and generally observed phenomena in DDT are given in Ref. 1.

Convective burning inside a solid propellant crack has been a subject of interest in recent years. An extensive literature review was conducted by Bradley and Boggs.[2] Both theoretical and experimental studies in this area have been conducted at The Pennsylvania State University.[3-5] It is known that cracks inside solid propellant grains, which are likely to be encountered in propellants with high solids loading, can allow hot, high-pressure gases to penetrate the cavity. The combustion processes inside the crack can produce much higher pressure than the designed maximum operating pressure. If the local pressure rise due to the gasification is sufficiently rapid, it may produce strong compression waves, or even shock waves which can initiate detonation.

Presented as Paper 79-1175 at the AIAA/SAE/ASME 15th Joint Propulsion Conference, Las Vegas, Nev., June 18-20, 1979; submitted Aug. 13, 1979; revision received Dec. 10, 1979.

Index categories: Combustion Stability, Ignition, and Detonation.

*Graduate Student, Dept. of Mechanical Engineering. Student Member AIAA.

†Associate Professor, Dept. of Mechanical Engineering. Associate Fellow AIAA.

Convective burning, however, is not the only mechanism responsible for producing the steep pressure gradients that lead to the transition to detonation. Other mechanisms may also be important in DDT processes. The presence of numerous ignited spots and ablating surfaces at some distance from the combustion zone in a damaged propellant may enhance the possibility of DDT. The ignited spots can be produced by reflection of shock-like compression waves at the propellant surface located in the region ahead of the combustion zone. A similar phenomenon was observed during the course of experimental investigations of ignition and flame spreading inside a solid propellant crack. As noted in Ref. 5, under rapid pressurization rates ($\sim 10^5$ atm/s), anomalous ignition was observed near the crack tip region. High-speed ($\sim$ 15,000 pictures/s) motion picture films used to record the experimental observations of the flame propagation inside the crack show that, at high chamber pressurization rates, the tip region of the crack ignites before the convective ignition front propagates from the crack entrance to the tip. Consequently, under these operating conditions, two flame fronts moving in opposite directions have been observed: one propagates from the crack entrance and the other from the crack tip.

Under rapid pressurization conditions, ignition may be achieved near the crack-tip region—far ahead of the convective combustion zone in an isolated crack. It is conceivable that in the combustion of a prefractured or granulated propellant, numerous ignited regions can be generated in a similar manner by rapid rates of gasification and pressurization in the combustion zone. These ignited regions can propagate further to produce even higher gasification rates in the combustion chamber or in an actual rocket motor. Flame-front propagation rates can be increased not only by the presence of these ignited regions, but also by the steepening of compression or shock waves near the flame front; eventually, the waves become strong enough to initiate a final transition to detonation. Therefore, a fundamental understanding of the basic mechanisms that contribute to the generation of these ignited regions would be an important step in the convective burning and DDT study.

An extensive literature survey was undertaken to help identify the mechanisms responsible for crack-tip ignition. The heat transfer mechanism near the closed end of a long isolated pore, with a time-varying interface temperature, has not been studied in the past. Some of the published results, which are related to the problem being considered, are discussed in the following paragraphs.

McAlevy et al.[6,7] studied the mechanism of ignition of composite solid propellants by hot gases in a shock tube. The objectives of their study were: to measure the ignition delays of test propellants heated by a shock wave, to develop a theoretical model based upon the gas-phase ignition mechanism in order to calculate the ignition delay, and to study the effect of oxygen concentration on the ignition delay. For experimental measurements, the specimen was flush-mounted in the end wall of a shock tube. The propellant was heated by high-temperature, high-pressure, stagnant gas behind the reflected shock wave. Photocells were used to detect ignition. In the theoretical model, it was assumed that, at the instant of shock reflection, a stagnant column of hot gases comes in contact with the propellant surface. The temperature of this column of gas was obtained from the reflected shock relationships. The interface temperature, which remains constant with time, was obtained by considering two uniform-temperature, semi-infinite bodies brought in contact at the instant of shock reflection. Pyrolized fuel vapor generated at the propellant surface propagates upstream at a rate governed by the laws of mass diffusion. This fuel vapor reacts with the gaseous oxygen and ignition results.

McAlevy et al. concluded that the observed ignition delay is the time required for sufficient fuel to react with the gaseous oxygen. The ignition delay time was found to increase with the decrease in oxygen concentration and pressure. Since this was the first study on the gas-phase ignition model, the analytic model has several limitations.[8] The assumptions of constant propellant surface temperature condition is not very realistic. Based upon their model, the calculated ignition delay time was an order of magnitude higher than the experimentally observed ignition delay. Contrary to their theoretical predictions, they observed a longer (two times) ignition delay for pure fuel than for composite propellant with the same fuel.[6,7]

Hermance et al.[9] improved the gas-phase ignition model by including oxidizer species equations. Later, they proposed a more realistic model for pure fuel[10] which included the effect of heat feedback to the propellant surface. Unfortunately, they did not make comparisons with the experimental data and, therefore, no conclusions can be drawn about the quantitative prediction capabilities. Although the effect of oxygen concentration (as observed by McAlevy et al.[6,7]) supports the concept of gas-phase ignition, there remains a large number of uncertainties and unknowns which could strongly influence the quantitative predictions of ignition delay. Some of these are: detailed processes involved in fuel and oxidizer pyrolysis, gasification temperatures of various ingredients in the propellant, the effect of exothermic oxidation at the propellant surface, and the catalytic effect of oxidizer gases on the vaporizing propellant surface. Because of these reasons, and because of the fact that the studies were conducted for shock tube conditions in which the effect of pressurization rates cannot be observed, the results of their ignition model cannot be used for the present study. Further improvements of the gas-phase ignition model and its application under shock tube operating conditions were made by Kumar and Hermance.[11-13]

Fay and Kemp[14] predicted the heat transfer rates to the end wall of a shock tube. In their analysis, the end wall of a shock tube was assumed to be suddenly put into contact with the quiescent hot gas. The pressure of the gas behind the reflected shock was determined from shock relationships. Continuity and energy equations in the gas phase were used. The wall was assumed to remain at its initial temperature. By using an integral method, a similarity type of solution was obtained for the heat transfer rate to the end wall. A closed form solution was obtained; this predicted the heat flux as a function of shock velocity and time. For the following reasons, results obtained from this study cannot be used to predict the heat transfer rate in the present study: a shock tube type of study cannot take into account the effect of pressurization rates; the end wall temperature is assumed to be at its initial constant temperature and, therefore, is not realistic for ignition studies; the rate of heat transfer to the end wall can only decrease with time ($\dot{q}_w \sim 1/\sqrt{t}$) in their analysis (this is true for their study, but is contrary to the physical situation of the present investigation).

Levy and Potter[15] made some transient measurements in a rarefaction wave tube. Their objectives were to build and calibrate a heat transfer instrument, to perform transient heat flux measurements in a rarefaction wave tube, and to evaluate the significant parameters which influence the instrument performance in the measurement of the transient heat flux. Using a heat transfer measuring instrument, they experimentally measured the heat transfer from the end wall for various pressure ratios. In their theoretical approach, they used energy and continuity equations in a control volume very close to the end wall. Temperature of the end wall was assumed to be constant, and the gas temperature variation was assumed to be a second-order polynomial of the distance from the end wall. The expansion process was assumed isentropic. From their analysis, they found that $\dot{q}_w/\sqrt{P_{\text{initial}}/P_{\text{atm}}}$ was a function of a dimensionless time ($tc_{\text{initial}}/L_{\text{tube}}$). This analysis has very limited use for the present study because of several simplifying assumptions and the physical process of depressurization.

Chao[16] offered an alternative approach to the same problem solved by Levy and Potter. Using an analytic solution, Chao solved the energy and continuity equations for an ideal gas. The end wall was assumed to remain at its initial temperature. Gas density was assumed to be independent of the axial location. By using a coordinate transformation, the energy equation for the gas phase was converted into the form of a heat equation. A closed-form solution for the dimensionless heat flux was obtained. The predicted heat transfer rate was in close ageement with the data of Levy and Potter. Once again, the assumption of constant end wall temperature and the physical process of depressurization makes this analysis of very limited use to the present study.

It is clear from the above literature survey that there has been no study, experimental or theoretical, which relates the combustion or the heat transfer phenomena at the closed end of a long channel to the rate of pressurization. It should also be noted that none of the existing theoretical models can be directly employed to study the current ignition phenomenon observed. Therefore, an experimental and theoretical study was undertaken with the following objectives:

1) To identify the important mechanisms responsible for the ignition of the crack tip.

2) To determine experimentally the dependence of the ignition delay time upon the pressurization rate.

3) To develop a theoretical model to predict the tip ignition phenomenon, in order that the opposing flame spreading process could be explained.

II. Possible Ignition Mechanisms

Before discussing the ignition mechanism, it is appropriate to define ignition. There is no single definition of ignition. It is often defined as the onset of emission of luminous light from a heated propellant surface; this usually occurs at the onset of ablation. However, this instantaneous emission of light and the gasification process may not continue once the stimulus is removed. Alternately, ignition is defined as the attainment of sustained burning even when the stimulus is removed. Depending upon the propellant ingredients and the ablation temperatures of the oxidizer crystals and fuel binder, the ignition delay times derived from these two definitions could differ significantly. This is especially true for nitramine propellants. In the special case in which the ablation temperatures of the oxidizer and fuel are almost identical (propellant A, used in this study, is an example), the ignition delay time associated with the onset of first light at ablation may be very close to that associated with sustained ignition. In the experimental portion of this study, therefore, ignition is defined as the onset of emission of luminous light from the propellant surface and, in the theoretical model, it is defined as the attainment of a critical temperature at the propellant surface.

The observed ignition (bright spot) of the tip region of the crack, before the arrival of the convective ignition front, can be attributed to one or more of the following mechanisms:

1) Turbulent diffusion of the hot product gases to the crack-tip region, and stagnation heating of the propellant by the hot gases at the crack tip.

2) Compression/shock wave heating of the gas adjacent to the propellant surface, and the stagnation heating of the propellant by the hot gases at the crack tip.

3) Ignition of combustible species evaporated from the propellant surface near the crack entrance region and transported to the propellant tip by the initial pressure gradient.

4) Ignition or combustion of the unreacted species from the igniter system carried to the crack tip by the initial pressure gradient.

5) Radiative heating of the crack tip.

6) Vaporization of the fuel binder at low temperatures, followed by a gas-phase reaction between the fuel and the oxidizer gases in the air near the crack-tip region.

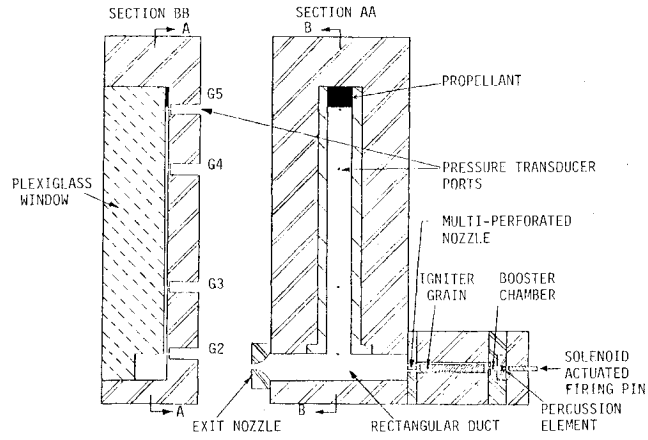

Fig. 1 Schematic diagram of combustion chamber.

Ignition near the tip region can be achieved if some of the combustible species evaporate from the propellant surface near the entrance of the crack, and if these species are transported by the initial pressure gradient to the crack-tip region, where they react and ignite. Under these circumstances, it is possible to observe the ignition of the tip region prior to the arrival of the convective ignition front. In order to investigate this possibility experimentally, an inert crack was formed (similar to that shown in Fig. 1, details of which will be discussed in the next section). It was designed to have inert surfaces along the crack, with a propellant sample only at the tip. The crack was formed between a thick plexiglass window and the bottom surface of the crack combustion chamber. To examine any material loss of the propellant at the tip, go/no-go tests were conducted for such a configuration. In all of the tests, the propellant sample burned and mass loss were observed. Since the tests were performed for the inert crack, it is impossible for any combustible species to evaporate from the crack entrance and then react at the tip. Therefore, it was possible to rule out the third mechanism mentioned above. Tests were also conducted with inert material (e.g., silicon rubber or clay) instead of propellant at the tip of the inert crack. High-speed motion pictures of these tests did not reveal a bright spot near the tip region, thereby eliminating the possibility of the reaction of some of the combustible species from the igniter system (the fourth mechanism).

These observations confirm the fact that the previously observed and reported[5] bright spot in a propellant crack is not caused by further reaction of fuel and oxidizer species resulting from the incomplete combustion of the propellant near the entrance region of the crack or from the igniter system. The bright spot represents the actual ignition of the propellant at the crack tip.

Some preliminary calculations were made to evaluate the effect of radiative heating. Calculations showed that radiative heating of the propellant at the tip by the hot gases in the combustion chamber is far too low to cause ignition. One of the main reasons for such a small amount of radiative heating is that the crack length to hydraulic diameter ratio is in the order of 80, resulting in a very small shape factor. Therefore, the fifth mechanism mentioned above was eliminated.

The sixth mechanism, i.e., the gas-phase reaction mechanism, is quite probable, especially for propellants using fuel with low vaporization temperatures. However, the gas-phase reaction may not be appreciable for propellants with fuel binders having high vaporization temperatures (i.e., those which are nearly identical to the vaporization temperature of the oxidizer crystals). Propellant A, for which all tip ignition experiments were conducted, is an example of the latter type; its fuel binder and oxidizer have almost identical vaporization temperatures. For the present study, therefore, the gas-phase ignition mechanism may not play an important role and hence is not considered here. It should be noted,

however, that the gas-phase reaction mechanism may be important for other types of propellants. This leaves only the first two possible mechanisms to be considered for crack-tip ignition. The ignition could be caused by a combination of these two mechanisms.

III. Experimental Investigation

Numerous experimental test firings were conducted to obtain the effect of pressurization rates on the ignition delay time. Propellant A was the test propellant used in all tip ignition tests. A schematic diagram of the combustion chamber is shown in Fig. 1. The rectangular cross-sectional channel simulating the crack was placed normal to the flow direction in the chamber. A pair of brass strips was placed between the bottom surface of the combustion chamber and the innermost plexiglass window to form the crack. The gap width of the crack thus formed was 1.3 mm. The length of the cracks was about 190 mm and the width was 9.4 mm. The plexiglass window was used as one of the surfaces of the channel to facilitate unobstructed viewing of the ignition phenomena. The chamber was completely sealed, except for the interchangeable exit nozzle through which the product gases were discharged to the atmosphere. The chamber was designed for a maximum static pressure of 800 atm. In this study, however, the maximum pressure was only about 200 atm.

A solid propellant igniter system was the source for hot gas generation. Percussion primers were used as the initiators for ignition of a propellant strand. A solenoid-activated firing pin triggered the primer. When the primer is triggered, the hot gases flow over the propellant strand and ignite it. The product gases flow through a multiperforated converging nozzle into the main chamber. The pressurization rate of the chamber can be varied by altering the dimensions of the propellant strip in the igniter, by changing the dimensions of the multiperforated nozzle, or by changing the exit nozzle of the chamber. In the present study, pressurization rates up to 8×10^4 atm/s were obtained at the crack tip.

The discharge of the product gases from the igniter system pressurizes the chamber, causing hot ignition gases to penetrate the crack cavity. The pressure wave fronts move along the crack, and are reflected from the solid propellant sample at the closed end. As soon as the hot gases reach the region near the closed end of the crack, heat begins to flow into the propellant surface and, consequently, the surface temperature rises. As the pressure in the chamber increases further, additional hot gas is driven into the crack. Depending upon the pressure gradient, the flow can be highly turbulent. Associated with the turbulent flow, there are temperature, density, and pressure fluctuations. The fluctuations can significantly increase the rate of heat transfer to the propellant. Finally, the ignition condition is realized and the propellant starts to burn.

A block diagram of the remotely controlled ignition and high-speed photography system is shown in Fig. 2. The solenoid which triggers the percussion primer is activated by an event switch built into the high-speed camera. After the camera is switched on, a few milliseconds are required to reach the desired framing rate. This delay time can be related to the footage of the film that passes through the camera before the attainment of the prescribed framing rate. The event switch is controlled by a footage indicator. During operation, the footage indicator is set to a preselected value corresponding to the desired framing rate. After a specified length of film (present on the footage indicator) runs through the camera, the event switch closes, and the relay is activated. The relay, in turn, activates two other switches; one switch triggers the solenoid to initiate the ignition event, the other closes the common-time switch on a light-emitting diode (LED) driver unit. At the instant at which the common-time switch closes, the LED driver unit generates a 2-ms pulse. The pulse is recorded on a magnetic tape and is simultaneously marked on the film. The common-time marks are used for the time correlation of the data recorded on the tape and film.

The data acquisition system consisted of two major parts: the pressure recording system and the ignition event recording system. A block diagram of the data acquisition system is shown in Fig. 3. Pressure measurements were taken at four locations along the crack, including one at the crack entrance and another at the tip. Piezoelectric quartz transducers (Kistler model 601 B) were used to measure the pressure. These transducers have a rise time of 1.5 μs, natural frequency of 300 kHz, and can accurately record pressures up to 1225 atm. The transducers were mounted in a water-cooled adapter

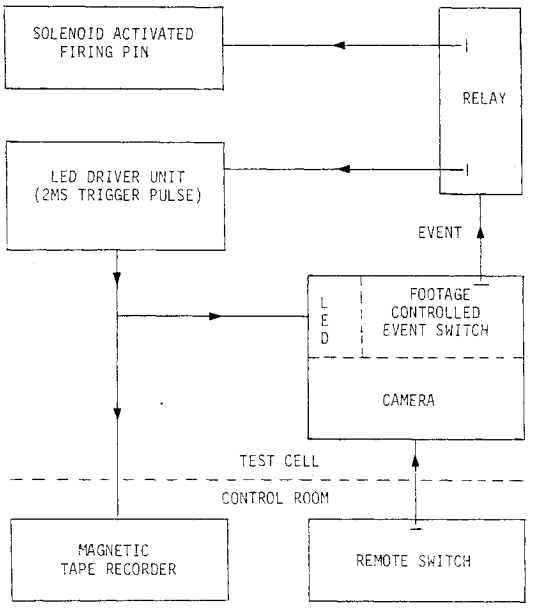

Fig. 2 Block diagram of remotely controlled ignition and photography system.

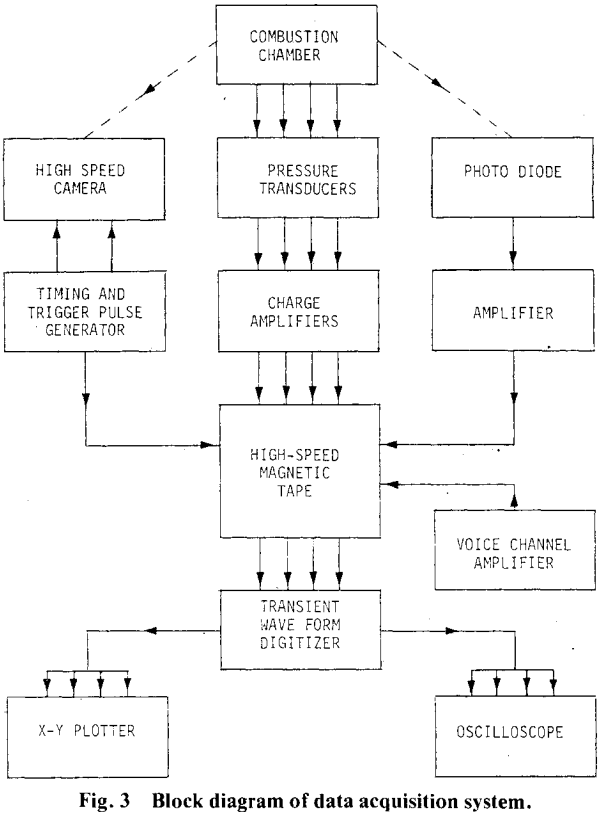

Fig. 3 Block diagram of data acquisition system.

(Kistler model 628 C), which prevented drifting or damage due to excessive heat. The signals from the pressure transducers were carried through an insulated, high-impedance, coaxial cable (Microdot model 121 M30), with a capacitance of 30 pF/ft, to a charge amplifier (Kistler model 504 E). The amplified signals were recorded on FM channels of a 14-channel AM/FM tape recorder (Hewlett-Packard model 3924B).

Two separate systems were used to simultaneously record the ignition event. A high-speed, 16-mm motion picture camera (Hycam model K20S4E-115) was used to observe the complete ignition event in the chamber. The camera was capable of filming at a maximum of 16,000 pictures/s. The Hycam unit is equipped with a dual LED timing system; this was used to record the common-time and timing marks on the film. The LED driver unit, a common-time pulse and high frequency (up to 10 kHz) timing generator, was used to operate the LED timing system. A photodiode system was also used to observe ignition at the tip. A camera lens (Schneider-Kreuznach 150 mm) was used to focus the tip region onto a photodiode (E.G. & G. model SGD040A). When the tip region is ignited, the photodiode gives out a signal which is amplified and recorded on the magnetic tape.

The data recorded on tape were digitized, using a 4-channel Biomation model 1015 waveform digitizer with a 1024-word memory per channel and a capability of maximum real time resolution of 10 μs. Output from the digitizer can be displayed on an oscilloscope (Tektronix type 535 A) or plotted on a x-y plotter (Hewlett-Packard model 7044A) for a hard copy.

A typical time-correlated experimental pressure trace is shown in Fig. 4. Even though pressures were measured at four axial locations, only those traces at the entrance and the tip are shown in the figure. The first discernible pressure rise for each pressure gage occurred consecutively from the crack entrance to the crack tip. The pressurization rates recorded at various gage locations along the crack indicate that the pressurization rates decrease consecutively downstream of the crack entrance. This attenuation can be attributed to the inert nature of the crack. A typical pressure-time trace at the tip can be divided into three regions: 1) the pressurization region, where the pressure continuously increases; 2) the constant pressure region; and 3) the depressurization region. The uprising portion of the pressure-time trace at the crack-tip location is quite linear. In most of the tests, the ignition occurred during the uprising portion of the pressure-time curve at the crack-tip location.

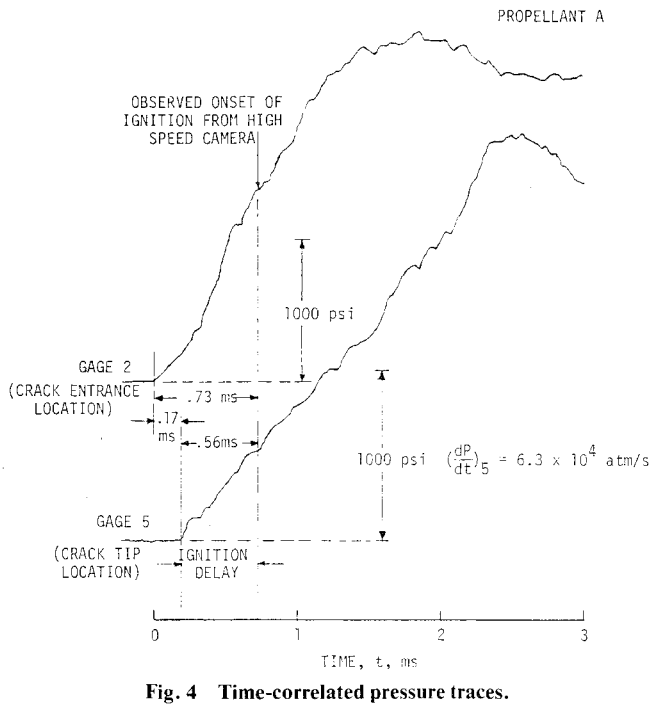

Fig. 4 Time-correlated pressure traces.

Ignition is defined in these tests as the onset of emission of luminous light from the propellant surface. The luminous light can be detected by either the high-speed motion picture camera or the photodiode. The high-speed camera was used for all tests; the photodiode system was used only during later tests. It was noted that the photodiode system alone cannot give a very reliable signal. This is because the photodiode picks up light reflected from the walls of the stainless steel combustion chamber even before the onset of ignition at the propellant tip. The high-speed motion picture made it possible to record a more complete ignition event, thereby reducing the possibility of error.

The common-time signal is omitted in the results presented in Fig. 4 because of a 4-5 ms time lag between the common-time signal and the first discernible pressure rise at the pressure gage located at the crack entrance. Since the region of interest is the uprising portion of the pressure traces, that region has been expanded; therefore, the common-time signal cannot be included in the same figure. The time-correlated pressure and ignition data indicated that the time of first discernible pressure rise coincides with the appearance of hot ignitier gases at the crack entrance. The time delay between the appearance of the hot igniter gases at the crack entrance and the ignition at the tip was obtained from the motion picture recording. The time lag between the first discernible pressure rises at the crack entrance and crack tip was obtained from the pressure-time traces. The difference between these time lags is the ignition delay time for the propellant at the tip. That is, the ignition delay time is the time lag between the arrival of the pressure wave at the tip and the incipient ignition. Ignition delay times are plotted against the pressurization rate at the tip (gage 5); no effort was made to relate them to pressurization rates at the crack entrance (gage 2).

IV. Theoretical Model

Mathematical Model Description

Since none of the existing theoretical models can be employed to study the observed tip ignition phenomenon, a theoretical model was developed to predict the ignition delay and its dependence upon the pressurization rate. The theoretical model considers an inert crack—a rectangular-shaped inert channel with propellant only at the tip. Ignition is defined as the attainment of a critical temperature at the propellant surface. It is assumed that no solid or gas-phase reaction takes place before the onset of ignition. Here, the tacit assumption is made that there is little time between the attainment of a critical surface temperature and the reaction between the fuel and the oxidizer species to cause ignition. For propellant A, the ignition of which is studied here, the surface temperature ignition criterion is quite suitable, since its fuel binders and the oxidizer have an almost identical vaporization temperature. It should be pointed out that if the fuel vaporization temperature is much lower than that of the oxidizer crystals, the gas-phase reaction between vaporized fuel and oxidizer in the ambient gas may be important, and that this ignition criterion may not be valid.

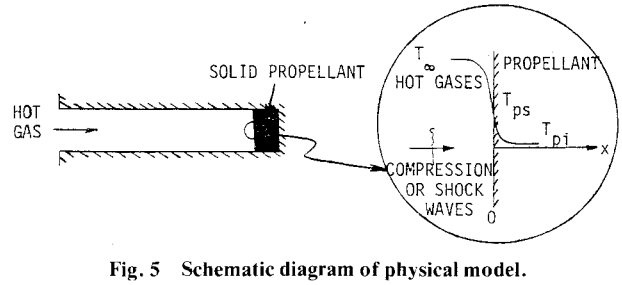

Fig. 5 Schematic diagram of physical model.

In the theoretical model, the propellant is considered to be a one-dimensional, semi-infinite solid which is brought in contact with hot gases at the instant of the arrival of the pressure front at the tip. The hot gases cause heat transfer to the propellant surface. A schematic diagram of the physical model considered is given in Fig. 5.

The solid-phase heat conduction equation is

$$\frac{\partial T_p}{\partial t} = \alpha_p \frac{\partial^2 T_p}{\partial x^2} \tag{1}$$

The initial and boundary conditions are

$$T_p(0,x) = T_{pi}$$

$$T_p(t,\infty) = T_{pi}$$

$$k_p \frac{\partial T_p}{\partial x}(t,0^+) = k \frac{\partial T}{\partial x}(t,0^-) = -\dot{q}_w(t) \tag{2}$$

where $\dot{q}_w(t)$ is the rate of heat transfer from the hot gases to the propellant surface and is unknown. In order to determine the heat flux at the propellant surface, the gas-phase equations must be considered.

Assuming the bulk flow to be predominatly one-dimensional, the transient mass and energy conservation equations are considered for the gas phase. Experimentally obtained pressure-time trace near the crack-tip region is used, instead of solving the pressure at the crack-tip through the use of momentum equation. The region of interest is that adjacent to the solid propellant surface. The governing equations can be written as follows:

Continuity:

$$\frac{\partial \rho}{\partial t} + \frac{\partial \rho u}{\partial x} = 0 \tag{3}$$

Energy:

$$\frac{\partial(\rho h)}{\partial t} + \frac{\partial(\rho u h)}{\partial x} - \frac{\partial P}{\partial t} - \underbrace{u\frac{\partial P}{\partial x}}_{\text{small}} = \frac{\partial}{\partial x}\left(k\frac{\partial T}{\partial x}\right) + \underbrace{\Phi}_{\text{small}} \tag{4}$$

dissipation

In order to simplify the analysis, the following basic assumptions are made:

1) $u(\partial P/\partial x) \ll (\partial P/\partial t)$ for the region of interest, i.e., locally uniform pressure near the propellant surface.
2) The viscous dissipation ϕ is small.
3) The specific heat c_p is constant.
4) The hot gases behave as ideal gas.

Using these assumptions and taking the Favre average[17] of the gas-phase conservation Eqs. (3) and (4), we get

$$\frac{\partial \bar{\rho}}{\partial t} + \frac{\partial}{\partial x}(\bar{\rho}\tilde{u}) = 0 \tag{5}$$

$$\bar{\rho}\frac{\partial \tilde{h}}{\partial t} + \bar{\rho}\tilde{u}\frac{\partial \tilde{h}}{\partial x} - \frac{\partial \bar{P}}{\partial t} = \frac{\partial}{\partial x}\left(\frac{\mu}{Pr}\frac{\partial \tilde{h}}{\partial x}\right) + \frac{\partial}{\partial x}\left(k\frac{\partial \overline{T''}}{\partial x} - \overline{\rho h'' u''}\right) \tag{6}$$

Considering $k(\partial \overline{T''}/\partial x)$ to be negligible in comparison with $\rho h'' u''$ and defining

$$-\overline{\rho h'' u''} \equiv \frac{\mu_t}{Pr_t}\frac{\partial \tilde{h}}{\partial x} \tag{7}$$

the energy equation can be written in the following form

$$\bar{\rho}\frac{\partial \tilde{h}}{\partial t} + \bar{\rho}\tilde{u}\frac{\partial \tilde{h}}{\partial x} - \frac{\partial \bar{P}}{\partial t} = \frac{\partial}{\partial x}\left(\frac{\mu}{Pr}\frac{\partial \tilde{h}}{\partial x} + \frac{\mu_t}{Pr_t}\frac{\partial \tilde{h}}{\partial x}\right) \tag{8}$$

The initial and boundary conditions are

$$\tilde{T}(0,x) = T_i$$

$$\tilde{T}(t,-\infty) = T_\infty$$

$$\tilde{T}(t,0) = T_p(t,0) \tag{9}$$

The equation of state is

$$\bar{P} = \bar{\rho} R \tilde{T} \tag{10}$$

Integrating the continuity equation (5), and using the boundary condition, $\tilde{u} = 0$ at $x = 0$, we get

$$\bar{\rho}\tilde{u} = \int_0^x -\left(\frac{\partial \bar{\rho}}{\partial t}\right) dx \tag{11}$$

Replacing the $\bar{\rho}\tilde{u}$ term in the gas phase energy equation (8) by Eq. (11), we get

$$\bar{\rho}\frac{\partial \tilde{h}}{\partial t} - \left[\int_0^x \frac{\partial \bar{\rho}}{\partial t} dx\right]\frac{\partial \tilde{h}}{\partial x} - \frac{\partial \bar{P}}{\partial t}$$

$$= \frac{\partial}{\partial x}\left[\left(\frac{\mu}{Pr} + \frac{\mu_t}{Pr_t}\right)\frac{\partial \tilde{h}}{\partial x}\right] \equiv \frac{\partial}{\partial x}\left(k_{\text{eff}}\frac{\partial \tilde{T}}{\partial x}\right) \tag{12}$$

At this point, in order to obtain the heat flux to the propellant surface and the propellant surface temperature, Eqs. (1) and (12) together with the boundary conditions [Eqs. (2) and (9)] must be solved simultaneously. An attempt was made to solve these equations analytically to obtain closed-form solutions for the propellant surface temperature. The partial differential questions can be transformed into a diffusion type of equation (see Ref. 4). Difficulties encountered in obtaining analytical solution are discussed in Ref. 4. In order to obtain theoretical results to compare with experimental data, this set of equations is solved numerically.

The region near the propellant surface is the most interesting, since it is here that large temperature gradients exist. For mathematical tractability, the infinite x region is transformed into a finite region, using the transformation given below. The transformed coordinate system also makes possible a finer grid size near the propellant surface in the real spatial coordinate, while using a uniform grid in the transformed coordinate.

For the gas phase region: $-\infty \le x \le 0$ can be transformed to $-1 \le z \le 0$ if we define

$$z = -\left[1 - \frac{1}{1 - Ax}\right] \tag{13}$$

After making these substitutions into the gas phase energy equation (12) and the initial and boundary conditions (9), plus some simplifications, we get

$$\frac{\partial \tilde{T}}{\partial t} = \left\{\left[\int_0^z \frac{\partial \bar{\rho}}{\partial t}\frac{dz}{(1+z)^2}\right]\frac{(1+z)^2}{\bar{\rho}}\right.$$

$$\left. + \frac{1}{\bar{\rho}}\left(\frac{\mu}{Pr} + \frac{\mu_t}{Pr_t}\right)2A^2(1+z)^3\right\}\frac{\partial \tilde{T}}{\partial z}$$

$$+ \left(\frac{\mu}{Pr} + \frac{\mu_t}{Pr_t}\right)\frac{1}{\bar{\rho}}A^2(1+z)^4\frac{\partial^2 \tilde{T}}{\partial z^2} + \frac{1}{\bar{\rho}c_p^c}\frac{\partial \bar{P}}{\partial t} \tag{14}$$

$$\tilde{T}(0,z) = T_i$$

$$\tilde{T}(t,-1) = T_\infty$$

$$\tilde{T}(t,0) = T_p(t,0) \tag{15}$$

For the solid phase region: $0 \le x \le \infty$ can be transformed to $0 \le z \le 1$ if we define

$$z = \left[1 - \frac{1}{1+A_1 x}\right] \tag{16}$$

After making these substitutions into Eqs. (1) and (2), plus some simplifications,

$$\frac{\partial T_p}{\partial t} = [-2A_1^2(1-z)^3\alpha_p]\frac{\partial T_p}{\partial z} + [A_1^2(1-z)^4\alpha_p]\frac{\partial^2 T_p}{\partial z^2} \tag{17}$$

$$T_p(0,z) = T_{pi}$$

$$T_p(t,1) = T_{pi}$$

$$Ak\frac{\partial \tilde{T}}{\partial z}(t,0^-) = A_1 k_p \frac{\partial T_p}{\partial z}(t,0^+) \tag{18}$$

Numerical Scheme

The coupled set of partial differential equations (namely, the energy equation for the fluid and the transient heat conduction equation for the propellant) was solved, using a finite-difference numerical technique. The most important solution parameter was the interfacial temperature as a function of time. The heat flux to the propellant surface was then easily computed from the calculated temperature distribution. The finite-difference equations were written for the equations in transformed coordinates. As mentioned in the previous section, this transformation made possible the use of uniform grid spacing in z coordinate, thereby bypassing the instability associated with nonuniform grid spacing, which would have been necessary for the x coordinate. The compression of the axis near the interface was controlled by parameters A and A_1. Larger values of A and A_1 result in finer grid spacing near the interface.

The two partial differential equations (14) and (17) to be solved are of the form

$$\frac{\partial T}{\partial t} = B(T,z)\frac{\partial T}{\partial z} + C(T,z)\frac{\partial^2 T}{\partial z^2} + D(T,z) \tag{19}$$

The backward difference method was used to approximate the time derivative and central difference for spatial derivatives. The equations were linearized by evaluating coefficients B, C, and D at an intermediate time step. When $T_i^k = T(k\Delta t, i\Delta x)$, Eq. (19) is approximated by

$$\frac{T_i^{k+1} - T_i^k}{\Delta t} = B_i^{k+\frac{1}{2}}\left[\frac{T_{i+1}^{k+1} - T_{i-1}^{k+1}}{2(\Delta z)}\right]$$

$$+ C_i^{k+\frac{1}{2}}\left[\frac{T_{i+1}^{k+1} - 2T_i^{k+1} + T_{i-1}^{k+1}}{(\Delta z)^2}\right] + D_i^{k+\frac{1}{2}} \tag{20}$$

The resulting set of simultaneous algebraic equations was solved by using a standard tridiagonal matrix inversion. At each time step, the properties at $k+\frac{1}{2}$ were evaluated, using linear interpolation between k and $k+1$ levels. Iteration was performed at each time step until the solution converged.

V. Discussion of Results

The input variables used in a typical run for the tip ignition program are given in Table 1. The computation is terminated when the propellant surface temperature reaches the specified ignition temperature of 850 K (this value was obtained from the sponsor and is based upon the best available data). Since no experimental or theoretical results are available in the literature for turbulent transport properties under highly transient flow conditions, the initial selection of k_{eff}/k was somewhat arbitrary. However, it was selected because of its close agreement with one measured ignition delay. In all later computations, the same value of k_{eff}/k was used. The parameter k_{eff}/k takes into account the effect of turbulent diffusion near the tip region, and includes the effect of secondary flow there. It also encompasses some heating effect of compression wave reflection at the crack tip. Both mechanisms will enhance the rate of heat transfer to the propellant surface. The rate of pressurization of the waves enters through the $\partial \bar{P}/\partial t$ term in the energy equation. It can be seen from Eq. (8) that when $\partial \bar{P}/\partial t$ is moved to the right-hand side, it acts as a source term in the energy equation. Thus, the model takes into account both of the first two possible ignition mechanisms listed in Sec. II.

Table 1 Input variables for tip-ignition computer program

$M_w = 26.10\ g_f/g\text{-mole}$	$T_{ign} = 850$ K
$\gamma = 1.21$	$T_i = 298$ K
$\rho_p = 1.71\ g/cm^3$	$T_{pi} = 298$ K
$k_p = 0.80 \times 10^{-3}$ cal/s-cm-K	$k = 2.085 \times 10^{-4}$ cal/s-cm-K
$\alpha_p = 0.0018\ cm^2/s$	$k_{\text{eff}}/k = 300$
$T_f = 3000$ K	$P_i = 1033.23\ g_f/cm^2$

Figure 6 shows the ignition delay as a function of the pressurization rate at the crack tip. This figure also shows the comparison of predicted and measured ignition delays. It can be seen that the ignition delay time decreases as the pressurization rate is increased. The slope of the curve is larger at the lower pressurization rates. The nature of the curve may help to explain why, at higher pressurization rates, the tip region of a real propellant crack may ignite prior to the arrival of the convective ignition front. At lower pressurization rates, the ignition delay time is much longer (>1 ms); therefore, the convective ignition front will reach the tip before the tip region ignites, due to stagnation point heat transfer associated with the compression waves and turbulent energy transport in the gas phase. However, as the pressurization rate is increased, the ignition delay time drops sharply, and under certain operating conditions, it may be smaller than the time required for the ignition front to propagate to the tip.

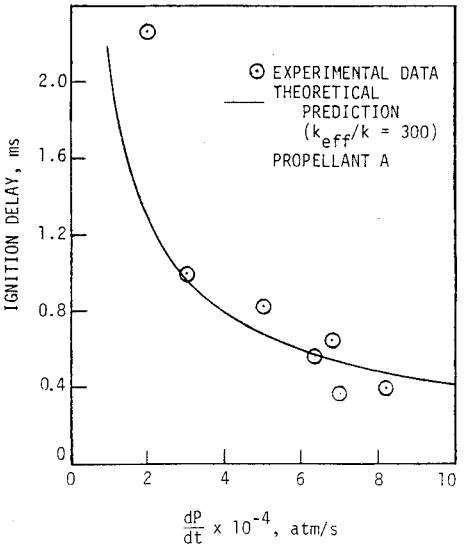

Fig. 6 Comparison of predicted and measured ignition delays.

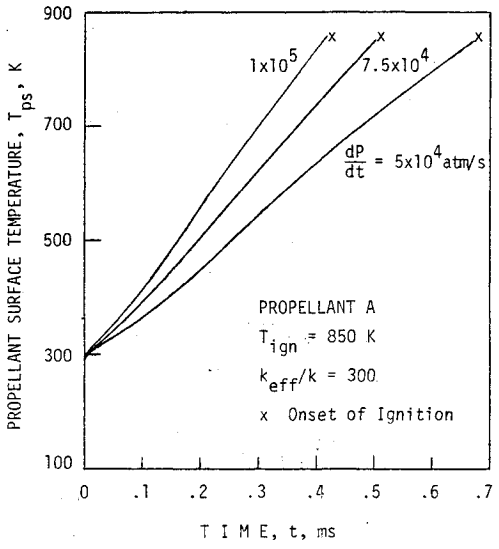

Fig. 7 Calculated propellant surface temperature vs time.

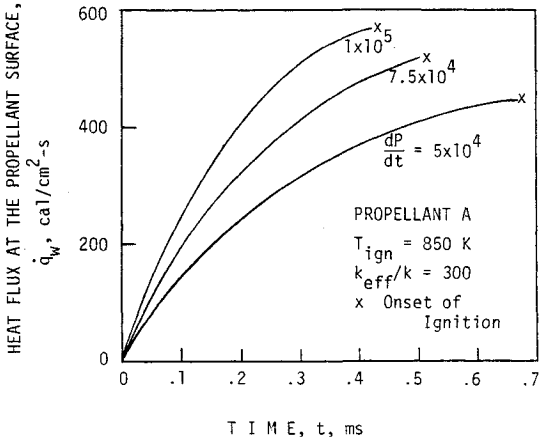

Fig. 8 Calculated heat flux vs time.

It should be noted that the numerical values of the ignition delay times and pressurization rates reported here should not be used arbitrarily for any crack geometry. The results for the tip ignition tests are for a given geometry; the numerical values of the results should, therefore, be used with caution. The theoretical predictions are also dependent upon the value of k_{eff}/k. An increase in this ratio will cause the ignition delay time vs pressurization rate curve to shift downward, whereas a smaller value of k_{eff}/k will cause it to shift upward. The validity of the theoretical model and the proposed physical mechanism is supported by good agreement between theoretical and experimental results.

Figure 7 presents a plot of predicted propellant surface temperatures as a function of time for pressurization rates of 5×10^4, 7.5×10^4, and 1×10^5 atm/s. The ignition delay time corresponding to these pressurization rates are 667, 503, and 411 μs. The propellant surface temperature increase is almost linear, although it shows some curvature at the beginning. As the pressurization rate is increased, the slope of the curve increases and, since the initial and the final temperatures for each case are the same, the higher pressurization rate results in lower ignition delay time. Even though the effect of initial propellant temperature is not discussed here, using the same argument it can be easily shown that higher initial propellant temperature will result in a smaller ignition delay time. The effect of pressurization rate on the heat flux to the propellant surface is shown in Fig. 8. For a given pressurization rate, the heat flux to the propellant surface increases with time. This is

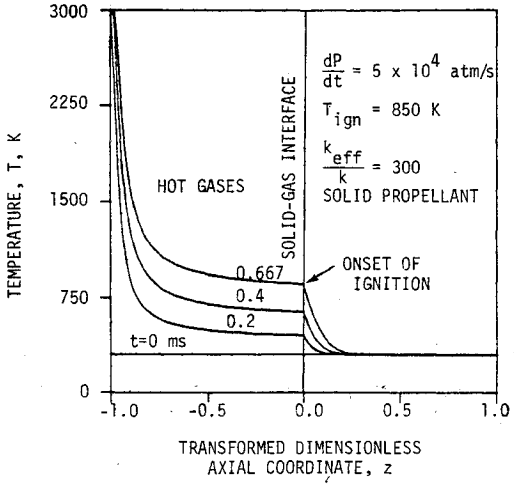

Fig. 9 Calculated temperature distribution at various times.

due to the pressurization of the crack by hot gases; the hot gases mix with the gases in the crack cavity, causing the temperature gradient at the propellant-gas interface to increase. As pressurization rate increases, the instantaneous heat feedback to the propellant also increases, causing the heat flux vs time curve to steepen.

The calculated temperature distribution at different times for a given pressurization rate is plotted in Fig. 9. The temperature is plotted as a function of the transformed dimensionless coordinate z, so that the detailed variations near the crack-tip region can be shown. The temperature profile in the solid propellant shows that the gradient $(\partial T/\partial z)_{z=0^+}$, which is proportional to $(\partial T/\partial x)_{x=0^+}$, steepens as time increases. The temperature gradients near the interface are steeper on the propellant side than are those on the fluid side, because the effective (turbulent plus molecular) thermal transport coefficient for the gas is higher than that of the propellant. Because of coordinate stretching, the high temperature region in the gas phase appears to be located at a considerable distance from the solid-gas interface. It should be noted that the distance of the high-temperature zone from the propellant surface is not the same as the flame standoff distance. It is merely the distance of the high temperature gas from the propellant surface at the onset of ablation.

VI. Summary and Conclusions

1) A theoretical model was developed to explain the tip ignition phenomena. It considers one-dimensional, unsteady mass and energy conservation equations for the gas phase near the crack tip. Experimentally observed pressure-time trace near the crack-tip region was used in place of a gas-phase momentum equation. A transient, one-dimensional heat conduction equation is considered for the solid phase.

2) A computer program was implemented, based upon the above theoretical model. It uses a stable, implicit scheme for the solution of the finite-difference equations. The program can predict ignition delay time, rate of heat flux to the propellant surface, temperature distribution, etc., as functions of pressurization rates.

3) Experiments were conducted in an inert crack to eliminate some of the possible mechanisms for the ignition at the tip. Test firings were conducted in the inert crack to obtain the effect of pressurization rate at the tip on the ignition delay time of the test propellant.

4) Both theoretical and experimental results of the tip ignition study indicate that the ignition delay time decreases as the pressurization rate is increased. Theoretically calculated ignition delay times are in good agreement with experimental data. Based upon this agreement, the ignition at the crack tip is believed to be caused by the enhanced turbulent energy

transport in the gas phase, which is driven by strong compression waves.

In view of the results of this study, the authors postulate that the observed ignition phenomena near the tip region could be one of the very important mechanisms responsible for the generation of ignited spots in a region ahead of the combustion zone. These ignited spots may cause rapid flame propagation in a discontinuous manner and may, therefore, contribute significantly to the DDT process.

Acknowledgments

This research has been sponsored by the Aerothermochemistry Division of the Naval Weapons Center, China Lake, Calif. The technical advice and support of R. L. Derr and C. F. Price are acknowledged. The help of A. S. Lundy, Los Alamos Scientific Laboratory, in the instrumentation is appreciated. The assistance of J. E. Wills and W. D. Jones of The Pennsylvania State University are also acknowledged.

References

[1] Price, E. W., ed., *Proceedings of ONR/AFOSR Workshop on Deflagration to Detonation Transition*, Atlanta, Fa., CPIA Publication 299, Sept. 1978.

[2] Bradley, H. H., Jr. and Boggs, T. L., "Convective Burning in Propellant Defects: A Literature Review," Naval Weapons Center, China Lake, Calif., NWC # TP 6007, Feb. 1978.

[3] Kuo, K. K., Chen, A. T., and Davis, T. R., "Convective Burning in Solid-Propellant Cracks," *AIAA Journal*, Vol. 16, June 1978, pp. 600-607.

[4] Kuo, K. K., Kumar, M., Kovacic, S. M., Wills, J. E., and Chang, T. Y., "Combustion Processes in Solid Propellant Cracks," Annual Report from The Pennsylvania State Univ., to the Naval Weapons Center, China Lake, Calif., 1979.

[5] Kuo, K. K., Covalcin, R. L., and Ackman, S. J., "Convective Burning in Isolated Solid Propellant Cracks," Naval Weapons Center, China Lake, Calif., NWC TP 6049, Feb. 1979.

[6] McAlevy, R. F., III, Cowan, P. L., and Summerfield, M., "The Mechanism of Ignition of Composite Solid Propellants," ARS Series on Progress in Astronautics and Rocketry, *Solid Propellant Rocket Research*, Vol. 1, Academic Press, New York, 1960, pp. 673-692.

[7] McAlevy, R. F., III, "The Ignition Mechanism of Composite Solid Propellants," Ph.D. Thesis, Princeton University, June 1960.

[8] Price, E. W., Bradley, H. H., Jr., Dehority, G. L., and Ibiricu, M. M., "Theory of Ignition of Solid Propellants," *AIAA Journal*, Vol. 4, July 1966, pp. 1153-1181.

[9] Hermance, C. E., Shinnar, R., and Summerfield, M., "Ignition of Hot, Stagnant Gas Containing an Oxidizer," *AIAA Journal*, Vol. 3, Sept. 1965, pp. 1584-1592.

[10] Hermance, C. E., Shinnar, R., and Summerfield, M., "Ignition of an Evaporating Fuel in a Hot Oxidizing Gas, Including the Effect of Head Feedback," *Astronautica Acta*, Vol. 12, March-April 1966, pp. 95-112.

[11] Hermance, C. E. and Kumar, R. K., "Gas Phase Ignition Theory for Homogeneous Propellants Under Shock Tube Conditions," *AIAA Journal*, Vol. 8, Sept. 1970, pp. 1551-1558.

[12] Kumar, R. K. and Hermance, C. E., "Ignition of Homogeneous Solid Propellants Under Shock Tube Conditions: Further Theoretical Development," *AIAA Journal*, Vol. 9, Aug. 1971, pp. 1615-1620.

[13] Kumar, R. K. and Hermance, C. E., "Gas Phase Ignition Theory of a Heterogeneous Solid Propellant Exposed to a Hot Oxidizing Gas," *Combustion and Science Technology*, Vol. 4, 1972, pp. 191-196.

[14] Fay, J. A. and Kemp, N. H., "Theory of Heat Transfer to a Shock-Tube End-Wall from an Ionized Monatomic Gas," *Journal of Fluid Mechanics*, Vol. 21, 1965, pp. 659-672.

[15] Levy, M. J. and Potter, J. H., "Some Transient Measurements in a Rarefaction Wave Tube," *Journal of Engineering for Industry, Transactions of ASME*, Ser. B, Vol. 86, Nov. 1964, pp. 365-370.

[16] Chao, B. T., "End-Wall Heat Transfer in a Rarefaction Wave Tube," *Journal of Heat Transfer*, Aug. 1965, pp. 349-352.

[17] Favre, A., "Equations des Gas Turbulents Compressibles," *Journal de Mechanique*, Vol. 4, 1965, pp. 361-390.